OPPORTUNITIES WITH ULTRA-SOFT PHOTONS: BREMSSTRAHLUNG FROM STOPPING*

Sohyun Park

Theoretical Physics Department, CERN, 1211 Genève 23, Switzerland

Received 1 August 2022, accepted 11 October 2022, published online 14 December 2022

We compute the spectra of bremsstrahlung photons for different stopping scenarios which give rise to different initial charge-rapidity distributions. In light of novel experimental opportunities that may arise with a new heavy-ion detector ALICE-3 at the CERN LHC, we discuss how to discriminate between these stopping scenarios and how to disentangle bremsstrahlung photons from other photon sources.

DOI:10.5506/APhysPolBSupp.16.1-A125

In the initial stage of ultra-relativistic nucleus–nucleus collisions, the electric charges of the incoming nuclei are significantly decelerated. This charge deceleration induces bremsstrahlung whose intensity is sensitive to the degree of longitudinal stopping. This has led to the idea of using bremsstrahlung from stopping to constrain the longitudinal charge distribution right after the collision [1–3]. Refined calculations of classical electromagnetic bremsstrahlung were carried out already in the late 1990s and they demonstrated that the effects are measurable [4–6]. In this regard, a dedicated detector at the BNL Relativistic Heavy Ion Collider (RHIC) was proposed [4] but it was never realized.

With our recent work [7] and with the additional calculations reported here, we aim to reassess the time-honored discussion of [1–6] for a different kinematic range at LHC and in light of the new experimental opportunities that the new ALICE-3 detector may offer in the coming decade [8]. In particular, this detector may give experimental access to ultra-soft photons with transverse momentum as low as 10 MeV at forward rapidity up to $y = 4$. As explained below, this is a potentially interesting kinematic range for the study of bremsstrahlung photons.

* Presented at the 29$^{\text{th}}$ International Conference on Ultrarelativistic Nucleus–Nucleus Collisions: Quark Matter 2022, Kraków, Poland, 4–10 April, 2022.

1. Classical bremsstrahlung

For an electric current $\boldsymbol{J}(\boldsymbol{x},t)$ that varies in space and time, the intensity of photons emitted with energy ω in direction $\boldsymbol{n}$ is given by the classical bremsstrahlung formula [9]

$$\frac{\mathrm{d}^2 I}{\mathrm{d}\omega\,\mathrm{d}\Omega} = |\boldsymbol{A}|^2\,, \qquad \boldsymbol{A}(\boldsymbol{n},\omega) = \int \mathrm{d}t \int \mathrm{d}^3x \boldsymbol{n}\times(\boldsymbol{n}\times\boldsymbol{J}(\boldsymbol{x},t))\,\mathrm{e}^{i\omega(t-\boldsymbol{n}\cdot\boldsymbol{x})}\,. \quad (1)$$

In heavy-ion collisions, up to the collision time $t = 0$, the electric charges move on the Lorentz-contracted pancakes of the incoming nuclei. We describe them by incoming currents $J_{\pm}^{(\mathrm{in})}(\boldsymbol{x},t)$, written in terms of the incoming charge density $Z\,e\,\rho_{\mathrm{in}}(r)$ in the transverse plane to the beam direction z times the beam velocity v_0,

$$J_{\pm}^{(\mathrm{in})}(\boldsymbol{x},t) = \pm\,\Theta(-t)\,Z\,e\,\rho_{\mathrm{in}}(r)\,v_0\,\delta(z\mp v_0 t)\,. \quad (2)$$

Here, $\boldsymbol{x} = (\boldsymbol{r},z)$, and we write the incoming velocity $v_0 = \tanh y_0$ in terms of the projectile rapidity $y_0 \simeq \ln\left(\frac{\sqrt{s_{NN}}}{m_N}\right)$. The entire electrical current $\boldsymbol{J}$ is the sum of the incoming ($t<0$) and outgoing ($t>0$) pieces, $\boldsymbol{J} = \boldsymbol{J}_{+}^{(\mathrm{in})} + \boldsymbol{J}_{-}^{(\mathrm{in})} + \boldsymbol{J}^{(\mathrm{out})}$. The outgoing piece $\boldsymbol{J}^{(\mathrm{out})}$ depends on the dynamics of stopping, *i.e.*, on the charge-rapidity distribution $\rho(\boldsymbol{r},y,t)$ right after the collision

$$J^{(\mathrm{out})}(\boldsymbol{x},t) = \Theta(t)\int_{-y_0}^{y_0} \rho(\boldsymbol{r},y)\,v(y)\,\delta\left(z - v(y)t\right)\,\mathrm{d}y\,, \quad (3)$$

where $-v_0 < v(y) = \tanh y < v_0$. Since the deceleration is primarily in the longitudinal direction, we consider the following electric-charge density distributions in which the longitudinal and transverse dependence factorizes, $\rho(\boldsymbol{r},y) = \rho_{\mathrm{in}}(\boldsymbol{r})\,\rho(y)$. The intensity of photons in Eq. (1) then can be written as

$$\frac{\mathrm{d}^2 I}{\mathrm{d}\omega \mathrm{d}\Omega} = \frac{\alpha Z^2}{4\pi^2}\sin^2\theta\,|F(\omega R\sin\theta)|^2\left|\left[\int \mathrm{d}y \frac{v(y)\rho(y)}{1-v(y)\cos\theta} - \frac{2v_0^2\cos\theta}{1-v_0^2\cos^2\theta}\right]\right|^2\,. \quad (4)$$

Here, the transverse form factor F is the Fourier transformation of charge density in the transverse plane

$$F(\omega R\sin\theta) = \int \mathrm{d}^2 r_\perp\,\rho_{\mathrm{in}}\left(r_\perp\right)\,\mathrm{e}^{-i\omega\boldsymbol{n}\cdot\boldsymbol{r}_\perp}\,, \quad (5)$$

which can be approximated by assuming that charges are distributed homogeneously in a sphere of radius R

$$F(q) = \frac{3}{q^2}\left(\frac{\sin q}{q} - \cos q\right), \qquad q \equiv \omega R \sin\theta\,. \tag{6}$$

This form factor becomes unity for a sufficiently small q. This means that the intensity is insensitive to the transverse profile of the charge distribution for sufficiently soft (small ω) and collinear (small θ) photons, *i.e.*, $q = \omega R \sin\theta \ll 1$. Indeed, the classical formula is valid for soft and collinear photons that do not resolve internal structure [7]. Hence, we work exclusively in the kinematic regime of $\omega < 200$ MeV, $\eta > 3$ which ensures $q < 1$.

2. Modelling the charge-rapidity distribution

The only unknown in the above set-up is the charge-rapidity distribution $\rho(y)$ in Eq. (4). The shape of $\rho(y)$ determines the bremsstrahlung spectrum and measuring this bremsstrahlung (or not measuring it but establishing a tight upper bound on it) constrains the allowed stopping scenarios $\rho(y)$. Here, we compare the five different models of charge-rapidity distribution depicted in Fig. 1. The total charge in the final state is $2 \times Z$, where Z is the charge number of the incoming nucleus. We adopt in the following a normalization where the integral over $\rho(y)$ is normalized to 2.

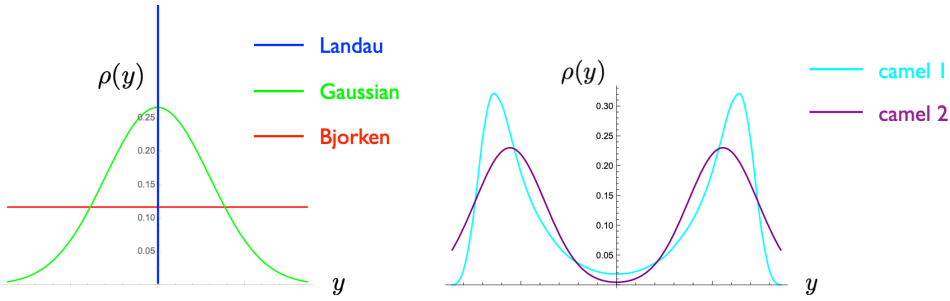


Fig. 1. (Colour on-line) Five different models of charge-rapidity distributions of net charge in a nucleus–nucleus collision referred to as (left panel) Landau (in blue/black), Gaussian (in green/light grey), Bjorken (in red/grey) in the left panel and camel 2 (in purple/grey) and camel 1 (in cyan/light grey) in the right panel.

3. Numerical results

Changing the kinematic variable in (1) from photon energy and angle (ω, θ) to transverse momentum and pseudo-rapidity (p_{T}, η), we determine the number of photons radiated per unit phase space

$$\frac{\mathrm{d}^2 N}{\mathrm{d}p_{\mathrm{T}}\,\mathrm{d}\eta} = \frac{2\pi}{p_{\mathrm{T}}\,\cosh^4\eta}\frac{\mathrm{d}^2 I}{\mathrm{d}\omega\,\mathrm{d}\Omega}\,. \tag{7}$$

Figure 2 shows the resulting p_{T}-differential bremsstrahlung spectrum with the characteristic soft $1/p_{\mathrm{T}}$ divergence and Fig. 3 shows the resulting number of photons per unit rapidity window in p_{T} bins of 10 MeV.

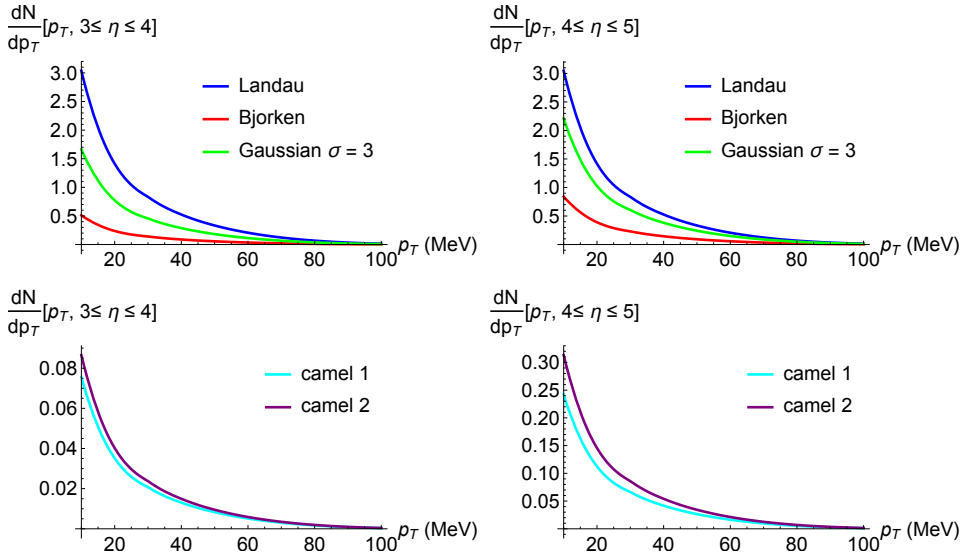


Fig. 2. The differential photon number spectrum as a function of p_{T} for different η bins.

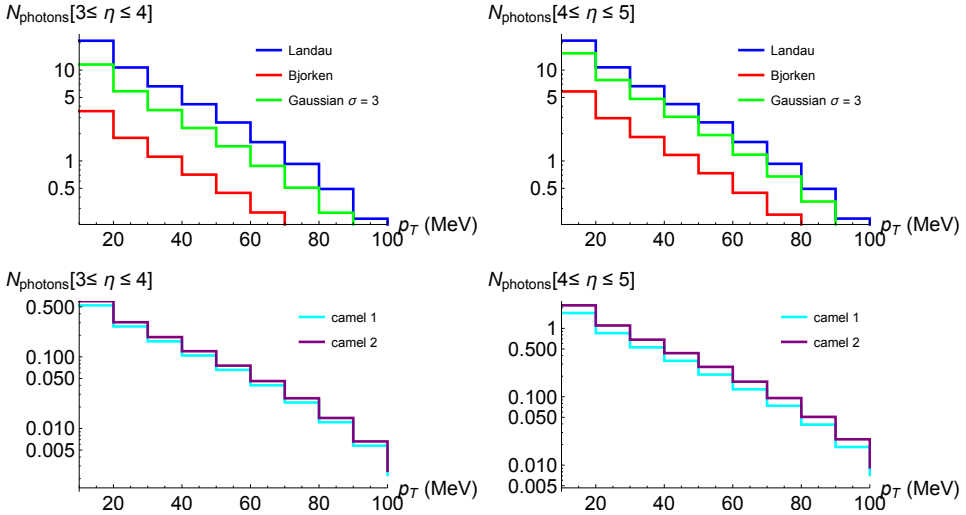


Fig. 3. The number of photons per unit rapidity window in p_{T} bins of 10 MeV.

The five stopping scenarios studied here map out different extremes: in the Landau scenario, all charges are maximally stopped and this scenario thus yields the largest photon bremsstrahlung intensity. The other four models (Gaussian, Bjorken, camel 2 and camel 1) correspond to scenarios in which less and less stopping occurs. In the limit in which $\rho(y)$ would correspond to two Kronecker delta's at rapidities $\pm y_0$, no stopping would occur and, therefore, no bremsstrahlung would be radiated. The camel 1 model comes the closest to this limiting case and it is therefore accompanied by the smallest photon bremsstrahlung intensity. Our numerical result quantifies this dependence.

4. Background photons

Photons from π^0-decays are expected to be the dominant background. For a rough estimate, we note that the $p_{\rm T}$-differential charged pion spectrum is almost flat for soft $p_{\rm T}$ at mid-rapidity: $\mathrm{d}N^{\pi^\pm}/\mathrm{d}p_{\rm T}\,\mathrm{d}y \simeq 2000/\mathrm{GeV}$ for $p_{\rm T} < 500$ MeV at $y = 0$ (read off from Fig. 21 of [12] which replots data from [13]). The η-differential charged pion spectrum $\mathrm{d}N_{\rm ch}/\mathrm{d}\eta$ decreases by roughly a factor of two from $\eta = 0$ to $\eta = 5$ in central PbPb collisions at the LHC (see Fig. 1 of [14]). Assuming π^0s have the same kinematic distribution as $\pi^\pm$s, we can estimate $\mathrm{d}N^{\pi^0}/\mathrm{d}p_{\rm T}\,\mathrm{d}y \simeq 500/\mathrm{GeV}$ for $p_{\rm T} < 500$ MeV and $4 < \eta < 5$. This amounts to five π^0s or equivalently ten background photons per event and per 10 MeV-bin of $p_{\rm T}$ at forward rapidity to be compared with the number of photons in Fig. 3. In other words, the signal-to-background ratio for the distributions in the upper panel of Fig. 3 is approximately

$$0.1 \lesssim \frac{S}{B} \lesssim 1 \quad \text{for} \quad p_{\rm T} \lesssim 50\,\mathrm{MeV} \quad \text{and} \quad \eta \gtrsim 3\,. \tag{8}$$

However, phenomenological models [10, 11] indicate that heavy-ion collisions are rather transparent to electric charge. A much better discrimination of bremsstrahlung signal to background is then required to establish bremsstrahlung photons. As seen from the left lower plot of Fig. 3, the experimental challenge of measuring bremsstrahlung for the stopping scenarios of [10, 11] amounts to identifying as little as 0.5 photons per event in the kinematic range $10\,\mathrm{MeV} < p_{\rm T} < 20\,\mathrm{MeV}$, $3 \le \eta \le 4$. This is experimentally challenging[1]. It, therefore, remains to be studied to what extent the experimental capabilities of future detectors like ALICE-3 can provide firm

[1] There are interesting parametric differences that may help to discriminate between bremsstrahlung photons and other photon sources. In particular,
— $p_{\rm T}$ dependence: $\frac{\mathrm{d}N^{\rm bgd}}{\mathrm{d}p_{\rm T}} \simeq \text{const.}$ *vs.* $\frac{\mathrm{d}N^{\rm brems}}{\mathrm{d}p_{\rm T}} \propto \frac{1}{p_{\rm T}}$,
— centrality dependence: $\frac{\mathrm{d}^2N^{\rm bgd}}{\mathrm{d}p_{\rm T}\mathrm{d}\eta} \propto N_{\rm part}$ *vs.* $\frac{\mathrm{d}^2N^{\rm brems}}{\mathrm{d}p_{\rm T}\mathrm{d}\eta} \propto Z^2 \propto N_{\rm part}^2$.

evidence for photon bremsstrahlung or whether they can only put experimental upper bounds on the bremsstrahlung spectrum that may allow one to disfavour some stopping scenarios. What our calculations clearly identify is the physics interest in equipping the kinematic range of ultra-soft photons of $\mathcal{O}(p_{\mathrm{T}} \sim 10\ \mathrm{MeV})$ at forward rapidity with sensitive detectors. Our work is one of several recent works [15, 16] that point to the interest in more precise soft photon measurements at the LHC.

I thank Urs Wiedemann for the collaboration and for critical reading of this manuscript. I also thank Soyeon Cho, DongJo Kim, Min-Jung Kweon, Jürgen Schukraft, and Martin Völkl for useful questions and discussions during 2022 Quark Matter Conference and in preparation of this manuscript.

REFERENCES

[1] J.I. Kapusta, *Phys. Rev. C* **15**, 1580 (1977).
[2] J.D. Bjorken, L.D. McLerran, *Phys. Rev. D* **31**, 63 (1985).
[3] A. Dumitru, L.D. McLerran, H. Stoecker, W. Greiner, *Phys. Lett. B* **318**, 583 (1993).
[4] S. Jeon, J.I. Kapusta, A. Chikanian, J. Sandweiss, *Phys. Rev. C* **58**, 1666 (1998), arXiv:nucl-th/9806047.
[5] J.I. Kapusta, S.M.H. Wong, *Phys. Rev. C* **59**, 3317 (1999), arXiv:hep-ph/9903235.
[6] S.M.H. Wong *et al.*, *Phys. Rev. C* **63**, 014903 (2001), arXiv:hep-ph/0008119.
[7] S. Park, U.A. Wiedemann, *Phys. Rev. C* **104**, 044903 (2021), arXiv:2107.05129 [hep-ph].
[8] D. Adamová *et al.*, arXiv:1902.01211 [physics.ins-det].
[9] J.D. Jackson, «Classical Electrodynamics», *Wiley*, New York 1998.
[10] Y. Mehtar-Tani, G. Wolschin, *Phys. Rev. Lett.* **102**, 182301 (2009), arXiv:0811.1721 [hep-ph].
[11] Y. Mehtar-Tani, G. Wolschin, *Phys. Rev. C* **80**, 054905 (2009), arXiv:0907.5444 [hep-ph].
[12] G. Nijs, W. van der Schee, U. Gürsoy, R. Snellings, *Phys. Rev. C* **103**, 054909 (2021), arXiv:2010.15134 [nucl-th].
[13] ALICE Collaboration (B.B. Abelev *et al.*), *Phys. Lett. B* **736**, 196 (2014), arXiv:1401.1250 [nucl-ex].
[14] ALICE Collaboration (J. Adam *et al.*), *Phys. Lett. B* **772**, 567 (2017), arXiv:1612.08966 [nucl-ex].
[15] P. Lebiedowicz, O. Nachtmann, A. Szczurek, *Phys. Rev. D* **105**, 014022 (2022), arXiv:2107.10829 [hep-ph].
[16] S. Floerchinger, C. Gebhardt, K. Reygers, arXiv:2112.12497 [nucl-th].